PCCP

PAPER

View Article Online
View Journal | View Issue

Cite this: *Phys. Chem. Chem. Phys.*, 2017, **19**, 24458

Wormlike micelles *versus* water-soluble polymers as rheology-modifiers: similarities and differences†

Ji Wang,[ac] Yujun Feng,[*ab] Niti R. Agrawal[d] and Srinivasa R. Raghavan[d]

Received 23rd July 2017,
Accepted 4th September 2017

DOI: 10.1039/c7cp04962e

rsc.li/pccp

Wormlike micelles (WLMs) formed from surfactants have attracted much attention for their ability to thicken water in a manner similar to water-soluble polymers. It is known that WLMs are cylindrical filaments that can attain very long contour lengths (~few μm), akin to chains of polymers with ultra-high molecular weights (UHMWs). In this study, we aim to make a direct comparison between the thickening capabilities of WLMs and UHMW polymers. The chosen surfactant is erucyl dimethyl amidopropyl betaine (EDAB), a C_{22}-tailed zwitterionic surfactant known to form particularly long WLMs independent of salt. The chosen polymer is nonionic polyacrylamide (PAM) having an UHMW of 12 MDa. Both EDAB WLMs and the PAM show strong thickening capability in saline water at 25 °C, but the WLMs are more efficient. For example, a 1.0 wt% EDAB WLM sample has a similar zero-shear viscosity η_0 (~40 000 mPa s) to a 2.5 wt% PAM solution. When temperature is increased, both samples show an exponential reduction in viscosity, but the WLMs are more sensitive to temperature. Microstructural differences between the two systems are confirmed by data from small-angle neutron scattering (SANS) and cryo-transmission electron microscopy (cryo-TEM). As expected, the key differences are that the WLM chains have a larger core radius (R_{core}) and in turn, a longer persistence length (l_p) than the PAM chains.

Introduction

Wormlike micelles (WLMs)—also called thread-like or giant micelles—are elongated, flexible aggregates self-assembled from surfactant molecules in aqueous solution. Above a threshold concentration, WLMs overlap and entangle into a transient network, thereby imparting viscosity and viscoelasticity to the solution.[1,2] In this regard, WLMs are much like water-soluble polymers, which have historically been used as thickeners in various applications ranging from oil production to personal care products. Indeed, WLMs are currently being evaluated as alternatives to polymers for thickening water, especially in oilfield applications.[2,3] This has been made possible especially by the advent of WLMs based on surfactants with "long" alkyl tails—*i.e.*, at least C_{22} (erucyl). Compared to conventional WLMs (which are based on surfactants with C_{16} or shorter tails), WLMs from C_{22} surfactants have higher viscosities and even gel-like behavior at room temperature; moreover, these samples retain a high viscosity even at temperatures beyond 80 °C.[4–7] A systematic comparison between such WLMs and a typical water-soluble polymer would therefore be of both scientific and practical interest.

From a theoretical standpoint, differences between WLMs and polymers have been discussed in detail. The differences stem from the bonds in the two structures. In the case of polymers, monomers are connected by strong covalent bonds to form a chain. In WLMs, surfactants are self-assembled into chains by weak physical bonds (hydrophobic interactions). Thus, polymer chains are 'unbreakable' because they are held by strong bonds, while WLMs are dynamic structures that constantly break and re-associate. WLMs are often called living[8] or equilibrium[9] polymers for this reason. Both chains form entangled networks when added to water at sufficient concentration (provided the chains are sufficiently long). Both these networks are transient: *i.e.*, each network is intact at short timescales, whereas the chains relax and disassociate from the network at long timescales. Polymer chains relax from their network by reptation.[10] WLMs relax by reptation as well, but in addition, they have a second, faster mode of relaxation due to their constant breaking and reforming.[11] This means that, if the chains were of the same length, WLMs would relax faster than polymers, *i.e.*, the relaxation time (and hence the solution viscosity) would be much lower.

[a] *Chengdu Institute of Organic Chemistry, Chinese Academy of Sciences, Chengdu 610041, People's Republic of China*
[b] *Polymer Research Institute, State Key Laboratory of Polymer Materials Engineering, Sichuan University, Chengdu 610065, People's Republic of China. E-mail: yjfeng@scu.edu.cn*
[c] *University of the Chinese Academy of Sciences, Beijing 100049, People's Republic of China*
[d] *Department of Chemical & Biomolecular Engineering, University of Maryland, College Park, Maryland, 20742-2111, USA*

† Electronic supplementary information (ESI) available: Synthesis of polybetaines, additional dynamic rheology, Cole–Cole plots. See DOI: 10.1039/c7cp04962e

In practice, it is possible for WLMs to be much longer than typical polymer chains, which could mean a higher thickening power for WLMs. Estimates of WLM contour lengths L suggest that they can easily reach a few μm, which would be comparable to polymers of ultra-high molecular weights (UHMWs), *i.e.*, 10^6 Da or larger. In addition, WLMs are also much thicker than polymer chains – *i.e.*, since the micelles are cylinders, their cross-sectional or core radius R_{core} is ∼few nm, which is 10× larger than the atomic dimensions of polymer chains. The higher thickness also means that WLMs are more rigid, *i.e.*, their persistence length l_p is also expected to be 10× larger than that of polymers. WLMs are therefore placed in the category of semiflexible chains[12] whereas linear polymers are generally considered flexible.[13] Chains with higher l_p should also pervade a larger volume, which should also contribute to their thickening efficiency.

To our knowledge, a systematic comparison of WLMs and polymers as rheology-modifiers has not been performed yet, for various reasons. One main reason is that typical WLM systems are mixtures of surfactant and salt, and their rheology is greatly influenced by the type and concentration of salt. For example, the most-studied WLMs are based on C^{16}-tailed cationic surfactants combined with hydrotropic salts like sodium salicylate. In these systems, the solution viscosity goes through a maximum as a function of salt concentration, which is generally not observed in polymer solutions.[14,15] Such complex nonmonotonic trends occur in most charged WLM systems. While some analogies have been noted between charged WLMs and polyelecrolytes,[16,17] a comparison would be much easier to perform if charge effects could be ignored. An ideal comparison would be between a neutral, water-soluble, UHMW polymer[18] and WLMs from a nonionic or zwitterionic surfactant. This is the subject of the present study.

The motivation for our comparative study comes from our work on zwitterionic surfactants with ultra-long (at least C_{22}) tails. One such surfactant, erucyl dimethyl amidopropyl betaine (EDAB), has been shown to form very long WLMs. The structure of EDAB is shown in Scheme 1 and it has an erucyl tail (C_{22} with a *cis* double bond in the middle) and a betaine headgroup that has both a cationic and an anionic part. Because the headgroups are net neutral, EDAB WLMs are unaffected by the presence of salt, and are thus an ideal candidate for our study. Initially, we planned to do a comparison of EDAB WLMs with a structurally similar UHMW polymer, and we therefore synthesized poly-(2-(dimethyl)(3-(acrylamido))propyl ammonium acetate)(PDAPAA), a polybetaine polymer (Scheme 1). However, our PDAPAA (Fig. S1, ESI†) had a molecular weight of only around 1.9×10^5 Da (Fig. S2, ESI†), and therefore did not have appreciable thickening power. Thereafter, we shifted our attention to commonly-used nonionic polyacrylamide (PAM)[18] (structure in Scheme 1), which is commercially available at an UHMW of 1.2×10^7 Da. We show that both this PAM as well as EDAB WLMs are efficient thickeners of saline water (water with 500 mM NaCl added). There are systematic differences between the two systems in terms of their rheology, and we attempt to correlate these differences using microstructural characterization techniques like small-angle neutron scattering (SANS) and cryogenic transmission electron microscopy (cryo-TEM).

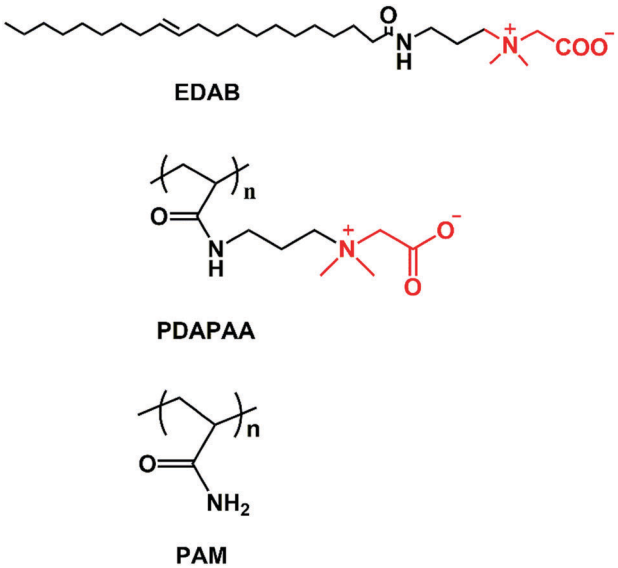

Scheme 1 Chemical structures of erucyl dimethyl amidopropyl betaine (EDAB), poly-(2-(dimethyl)(3-(acrylamido))propyl ammonium acetate) (PDAPAA) and polyacrylamide (PAM).

Experimental

Materials

The surfactant EDAB (Scheme 1) with a purity greater than 98.0% (Fig. S3 and S4, ESI†) was prepared following our previously-reported procedure.[19] The accompanied by-product NaCl content in EDAB was measured by ionic chromatography and found to be 1.03 wt% (Fig. S5–S7, ESI†). PAM was a commercial product kindly offered by Beijing Hengju Polymer Co., Ltd. The molecular weight of PAM is 1.20×10^7 Da.[20] Homogeneous solutions were obtained by separately adding EDAB or PAM powders into 500 mM NaCl aqueous solution, followed by mild heating at 40–50 °C and gentle agitation until the powders were completely dissolved. NaCl used in the experiments was analytical grade, and water was triply distilled by a quartz water-purification system. The resulting homogeneous sample solutions were stored at room temperature for at least 1 day prior to measurements.

Rheology

Rheological measurements were carried out on an MCR 301 (Anton Paar) rotational rheometer equipped with concentric cylinder geometry CC27 (ISO3219) with a measuring bob radius of 13.33 mm and a measuring cup radius of 14.46 mm. Sample solutions were equilibrated at the temperature of interest for no less than 20 min prior to experiments. Dynamic frequency spectra were conducted in the linear viscoelastic regimes, as determined from dynamic stress-sweep measurements. All experiments were carried out using stress-controlled mode, and Cannon standard oil was used to calibrate the instrument

before the measurements. The temperature was set to ±0.1 °C accuracy by a Peltier temperature control device, and a solvent trap was used to minimize water evaporation during the measurements.

Cryo-TEM

Sample specimens of EDAB and PAM solutions were prepared for cryo-TEM in a controlled-environment vitrification system. The climate chamber temperature was 25–28 °C, and the relative humidity was kept close to saturation to prevent evaporation from the sample during preparation. Two microliters of samples preheated at the desired temperatures (25 and 85 °C) were placed on a carbon-coated holey film supported by a copper grid and gently blotted with filter paper to obtain a thin liquid film (20–400 nm) on the grid. The grid was quenched rapidly in liquid ethane at −180 °C and then transferred to liquid nitrogen (−196 °C) for storage. Then the vitrified specimen was transferred to a Tecnai G^2 F20 cryo-microscope using a Gatan 626 cryo-holder and its workstation. The acceleration voltage was 200 kV, and the working temperature was kept below −170 °C. The images were recorded digitally with a charge-coupled device camera (Eagle) under low-dose conditions with an under focus of approximately 3 μm.

SANS

SANS measurements were made on the NG-3 (30 m) beamline at the NIST Center for Neutron Research (NCNR) in Gaithersburg, MD. Samples were studied in 2 mm quartz cells in a temperature-controlled chamber. The scattering spectra were corrected and placed on an absolute scale using calibration standards provided by NIST. The data are shown for the radially averaged, absolute intensity I *versus* the scattering vector $q = 4\pi \sin(\theta/2)/\lambda$, where λ is the wavelength of incident neutrons and θ is the scattering angle.

Results and discussion

Steady-shear rheology at room temperature

We characterized the thickening power of EDAB WLMs and PAM in saline water (*i.e.*, containing 500 mM NaCl) at 25 °C using steady-shear rheology. Results for PAM are shown in Fig. 1A and for EDAB in Fig. 1B. In the dilute regime, *e.g.*, 0.10% PAM and 0.01% EDAB, the samples show a Newtonian region at low shear-rate ($\dot{\gamma}$), where the viscosity is constant, followed by a region at high shear-rates (>100 s^{-1}) where the viscosity increases with shear rate, indicative of shear-thickening behavior. The shear-thickening seen for both WLMs and PAM solutions is likely an artifact due to Taylor instabilities.[21]

In the semi-dilute regime, take the cases of 2.50 wt% PAM and 1.00 wt% EDAB from Fig. 1A and B. Both exhibit Newtonian behavior at low shear-rates and shear-thinning response (*i.e.*, a decreasing viscosity) at high shear-rates. In the Newtonian regime, the constant value of the viscosity is termed the zero-shear viscosity (η_0). The high magnitude of η_0 reflects the presence of entangled networks of long chains in each sample. At low shear-rates, the applied deformation is too weak to disrupt this network. The onset of shear-thinning occurs at a critical shear rate ($\dot{\gamma}_c$); beyond this point, shear causes the chains to disentangle from the network and orient with the flow.[1,22] We note from Fig. 1A and B that both EDAB and PAM solutions can attain very high values of η_0 (~40 000 mPa s),

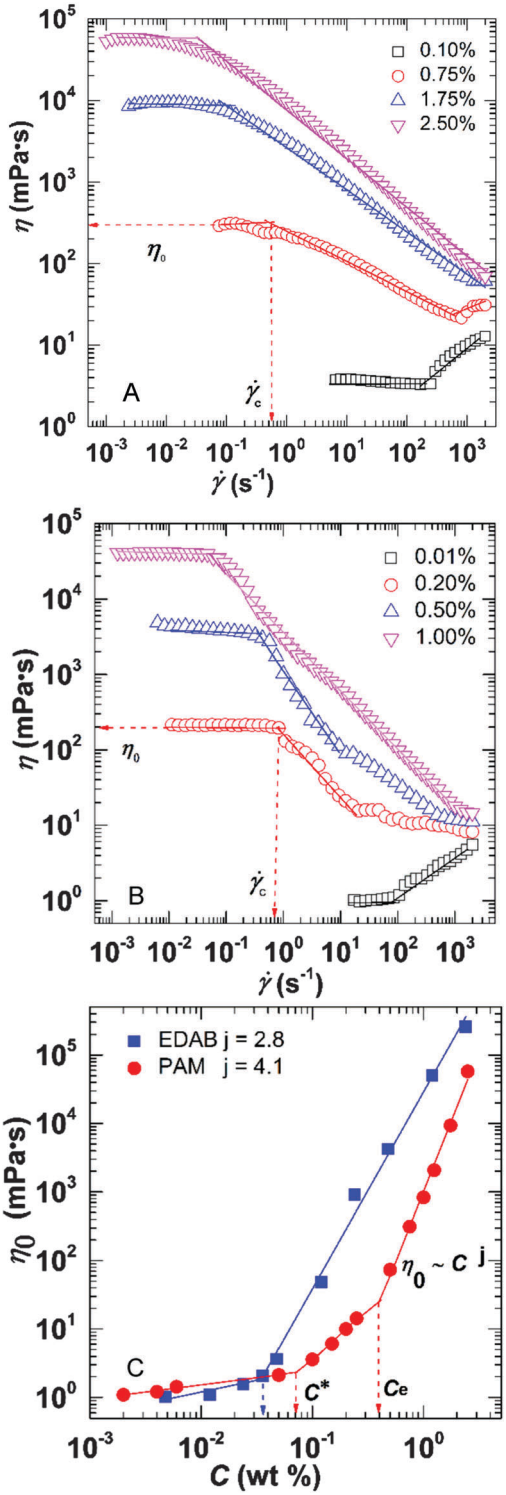

Fig. 1 Shear viscosity (η) plotted as a function of shear rate ($\dot{\gamma}$) for (A) PAM and (B) EDAB solutions at 25 °C; (C) variation of zero-shear viscosity (η_0) with concentration of PAM and EDAB at 25 °C.

but a lower amount of EDAB (1.00 wt%) is needed to reach this value compared to the PAM (2.50 wt%). Also, the transition from the Newtonian to the shear-thinning regime is sharper for the EDAB WLMs.

Fig. 1C shows the variation of η_0 with concentration for both systems at 25 °C. Note that a straight line on this log–log plot reflects a power-law scaling: $\eta_0 \sim C^j$ where j is the power-law exponent. The EDAB curve can be divided into two linear parts with a clear break-point at ~0.05 wt%. This is the critical overlap concentration (C^*), *i.e.*, the point at which adjacent WLMs first begin to overlap. Below C^*, η_0 shows a linear increase (j = 1) with concentration as the WLMs are unconnected (note that in the case of WLMs, the contour length L of the chains also tends to increase with concentration). Above C^*, the WLMs are overlapped and entangled into a network, leading to a much more rapid increase in η_0 (j = 2.8).

As for PAM, the curve can be divided into three parts with two clear break-points, *i.e.*, C^* (~0.1 wt%) and the entanglement concentration C_e (~0.5 wt%). In the dilute range ($C < C^*$), PAM chains are discrete structures and far from each other, leading to a weak increase in η_0 (j = 0.2). Thereafter, there is a range of concentrations corresponding to semidilute (*i.e.*, chains overlap), but unentangled polymer solutions ($C^* < C < C_e$), and here the viscosity begins to increase a bit more rapidly (j = 1.2). Above C_e, the polymer chains are entangled into a network, leading to a sharper increase in η_0 (j = 4.1). For comparison, note that the typical observation for linear, entangled polymer chains in a good solvent is j = 3.4.[23]

Dynamic rheology at room temperature

To compare the viscoelastic properties of EDAB and PAM solutions, we performed dynamic rheological scans at 25 °C on samples in the semidilute, entangled regime. In particular, samples of 2.50 wt% PAM and 1.00 wt% EDAB were chosen as representative because of their comparable viscosities from Fig. 1 ($\eta_0 \sim$ 40 000 mPa s). Fig. 2A shows the frequency spectra for the two above samples. It is clear that the PAM sample shows a viscoelastic response while the EDAB one shows an elastic one. That is, in the case of the EDAB sample, the elastic modulus (G') exceeds the viscous modulus (G'') over the frequency range and the moduli do not intersect. This implies that the samples are gel-like and have ultra-long relaxation times at 25 °C. The gel-like rheology of samples prepared from EDAB (as well as similar long-tailed surfactants) has been observed previously by both the Raghavan and Feng labs,[4–7] and is unusual in the context of WLMs. Typical WLM samples show a viscoelastic response at room temperature, but in the case of EDAB WLMs, such a response is only observed at high temperatures (see below for data).

As for the PAM solution, it shows a viscoelastic response that is qualitatively similar to that of typical worms, with elastic behavior ($G' > G''$) at high frequencies (ω) and viscous behavior ($G'' > G'$) at low ω. The viscoelasticity of the solution reflects the entanglement of long polymeric chains into a transient network. At high ω (short timescales), the network is intact, whereas at low ω (long timescales), the chains have sufficient

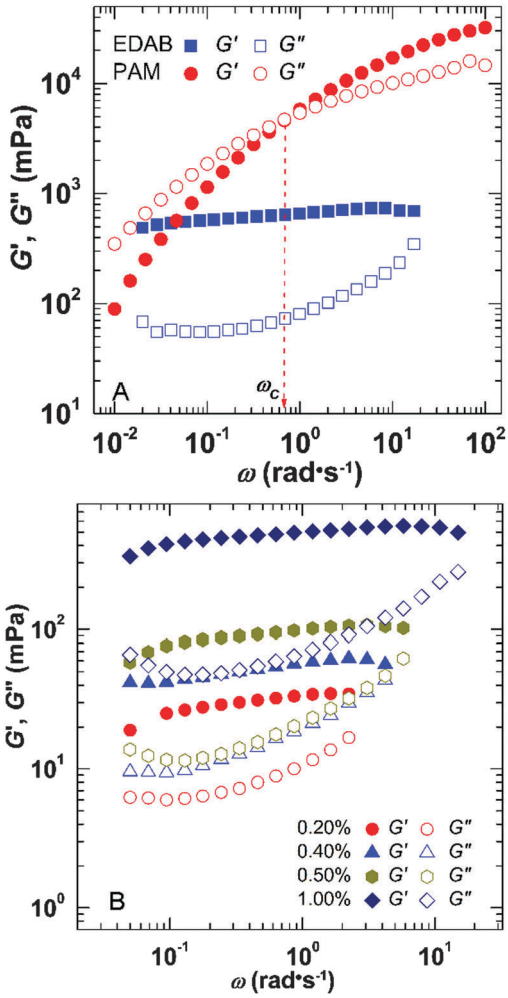

Fig. 2 Dynamic rheology for (A) 2.50 wt% PAM and (B) 1.00 wt% EDAB solutions at 25 °C.

time to disentangle and relax. Note that the PAM solution shows a spectrum of relaxation times rather than a single one; as a result, the G'–G'' data do not follow a semi-circle on a Cole–Cole plot (Fig. S8, ESI†). The crossover frequency (ω_c) defines the longest relaxation time τ_R:[12]

$$\tau_R = \frac{1}{\omega_c} \quad (1)$$

For the 2.50 wt% PAM solution, the τ_R from Fig. 2A is 1.6 s. In comparison, the τ_R for the 1.00 wt% EDAB solution is at least longer than 100 s (*i.e.*, outside the experimental window probed in the experiment).

Effect of temperature on rheology

We further compared the rheology of 2.50 wt% PAM and 1.00 wt% EDAB samples as a function of temperature. Data on the PAM sample under steady-shear rheology are shown in Fig. 3A and under dynamic rheology in Fig. 4A. Corresponding data on the EDAB sample are in Fig. 3B and 4B. The PAM solution shows a monotonic drop in low-shear viscosity with temperature. From the data, the zero-shear viscosity η_0 is extracted and

plotted in an Arrhenius plot (semi-log plot of η_0 *vs.* $1/T$) in Fig. 3C. The straight line on this plot shows that the data follow the relationship:

$$\eta_0 = A \exp\left(\frac{E_a}{RT}\right) \quad (2)$$

where A is a pre-exponential factor, E_a is the flow activation energy, R the gas constant, and T the absolute temperature. E_a can be calculated from the slope and its value is 24 kJ mol^{-1}. The reason for the decrease in η_0 with T is that the chains in the polymer network become more dynamic upon heating. As a result, they are able to relax out of this network more rapidly, *i.e.*, the relaxation time τ_R decreases with T; in turn, so does the η_0.

As for the EDAB WLMs, η_0 increases from 25 °C up to around 55 °C and thereafter decreases exponentially with temperature. The increase in viscosity at low temperatures has been seen before for WLMs based on other long-tailed surfactants (C_{22} or longer). A plausible explanation[4] is that, at 25 °C, some of the EDAB molecules may be sequestered in the micellar cores due to their hydrophobicity. When temperature is increased up to 55 °C, these molecules get solubilized, thereby increasing the concentration of EDAB WLMs. Beyond this temperature, the major effect of increasing T is that the micellar contour length L decreases exponentially. In turn, the shorter micelles relax more rapidly and thereby η_0 decreases exponentially. We again see a straight line for EDAB WLMs on the Arrhenius plot in Fig. 3C (for $T \geq 55$ °C). The flow activation energy E_a for EDAB from the slope of this line is 145 kJ mol^{-1}. Note that this is much higher than the E_a for PAM solutions, indicating that WLMs are much more sensitive to temperature than polymer chains.

We also compare the frequency response at 25 °C and 85 °C for the PAM (Fig. 4A) and the EDAB (Fig. 4B) samples. The PAM sample shows the same shape for G' and G'' at both temperatures. The only difference is that the data at 85 °C is shifted along the x-axis to higher frequencies, *i.e.*, the relaxation time τ_R is lowered at the higher temperature (its value is now reduced to 0.33 s). On the other hand, the EDAB WLM sample shows a drastic change in the shape of the spectra. While the response at 25 °C is gel-like (G' and G'' do not cross), the response at 85 °C is viscoelastic ($G' > G''$ at high ω and $G'' > G'$ at low ω). The viscoelastic behavior of WLMs is often known to follow the Maxwell model, as described by the following equations:[24]

$$G'(\omega) = \frac{G_0(\omega\tau_R)^2}{1 + (\omega\tau_R)^2} \quad (3)$$

$$G''(\omega) = \frac{G_0\omega\tau_R}{1 + (\omega\tau_R)^2} \quad (4)$$

Here, G_0 is the plateau modulus (*i.e.*, the constant value of G' at high ω) and τ_R is the relaxation time ($= 1/\omega_c$). For the EDAB solution at 85 °C, the viscoelastic response can be fit to the above equations (shown as lines) at low and intermediate ω, indicating that the sample is a Maxwell fluid with a single relaxation time.

The fact that a single τ_R exists for EDAB at 85 °C implies that the WLMs are now in the "fast-breaking" limit, *i.e.*, with each WLM chain breaking and re-forming rapidly even as the overall chain undergoes reptation. That is, when considering the timescales for chain reptation (τ_{rep}) and micelle breaking (τ_b), the fast-breaking limit corresponds to $\tau_b \ll \tau_{rep}$.[11] The single

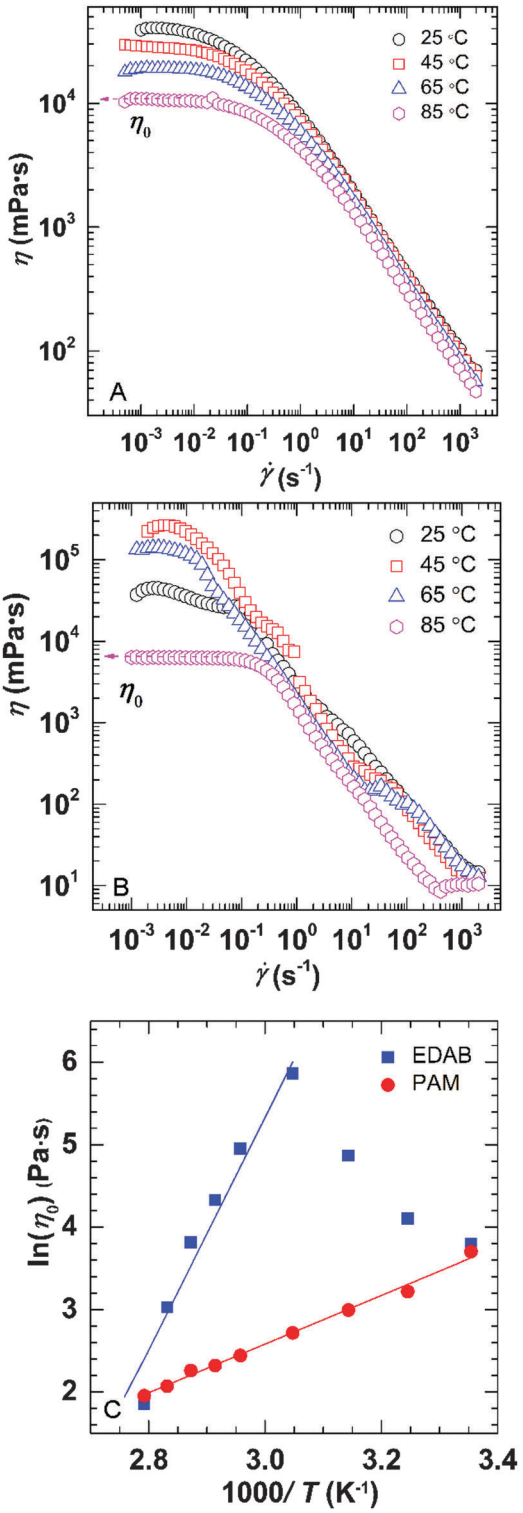

Fig. 3 Shear viscosity (η) plotted as a function of shear rate ($\dot{\gamma}$) for (A) 2.50 wt% PAM and (B) 1.00 wt% EDAB solutions at different temperatures; (C) arrhenius plots of ln(η_0) *vs.* $1/T$ for WLMs and PAM solutions. The solid lines are fits to the data.

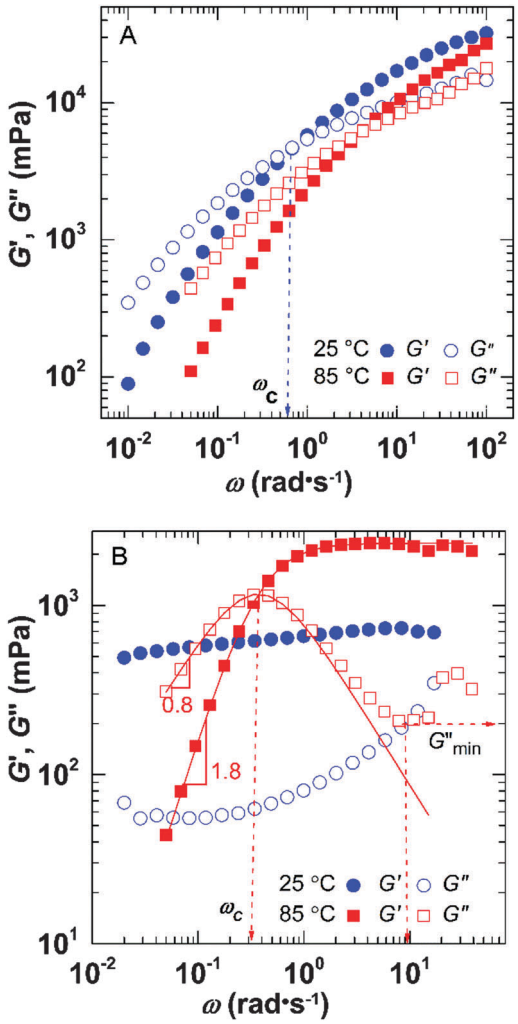

Fig. 4 Dynamic rheology for (A) 2.50 wt% PAM and (B) 1.00 wt% EDAB solutions at 25 and 85 °C, respectively. The lines (B) are fits to the Maxwell model (eqn (3) and (4)).

τ_R is then expected to be the geometric mean of the above timescales:[11,25]

$$\tau_R = \sqrt{\tau_b \tau_{rep}} \quad (5)$$

From the data in Fig. 4B, $\omega_c \sim 0.33$ rad s^{-1} giving $\tau_R \sim 3$ s. Regarding the breaking time τ_b, one estimate for it is from the frequency at which the viscous modulus G'' shows an upturn in Fig. 4B. This frequency is ~10 rad s, meaning that $\tau_b \sim 0.1$ s. In turn, from eqn (5), $\tau_{rep} \sim 90$ s.

Cryo-TEM studies

Cryo-TEM is a most useful technique for studying complex fluids. Samples are rapidly vitrified, thus preserving their at-rest microstructure.[26] Here, we used cryo-TEM to visualize the microstructures in a 1.00 wt% EDAB solution at 25 and 85 °C. Exhibited in Fig. 5A is a typical cryo-TEM image at 25 °C. Numerous cylindrical filaments (*i.e.*, WLMs) are observed, and these are entangled with each other. The WLMs appear to be a few nanometers in radius (R_{core}). The ends of individual WLMs

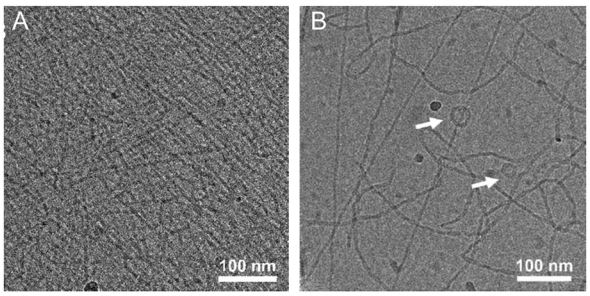

Fig. 5 Cryo-TEM micrographs of WLMs formed by 1.00 wt% EDAB at 25 °C (A) and 85 °C (B).

are not seen and therefore it is difficult to measure the WLM contour length L, but we can infer that L is at least several microns. No other types of structures are observed in the cryo-TEM images that could explain why EDAB samples show a gel-like rheology at low temperatures. Our cryo-TEM images of EDAB WLMs at 25 °C are consistent with those published previously on the same system.[4]

Fig. 5B shows a typical cryo-TEM image of the EDAB sample at 85 °C. Here, very long, entangled WLMs are again observed, with their diameters again being a few nanometers, and some reaching a length of several microns. However, there are fewer WLMs in this image compared to the one at 25 °C, which may imply that many of the original WLMs have been significantly reduced in length by the increase in temperature. Also, in addition to long straight filaments, we also see some branched structures as well as ring-like structures (10–20 nm in diameter), as indicated by the arrows. Overall, the data are consistent with a temperature-induced reduction in WLM size. Lastly, we also conducted cryo-TEM on the 2.50 wt% PAM solution at 25 and 85 °C, but the images (Fig. S9, ESI†) do not reveal any structural features. This is not surprising since the polymer chains are expected to have atomic dimensions, *i.e.*, less than a nanometer in radius, which is too small to be resolved by cryo-TEM.

SANS studies

To complement the cryo-TEM studies, we also used SANS to probe the microstructures in the WLM and polymer solutions. Samples of 1 wt% EDAB and 2.5 wt% PAM were made in D_2O to achieve sufficient contrast between the scattering objects and solvent. Fig. 6 plots the scattering intensity I *versus* wave-vector q for these two samples at temperatures of 25 and 85 °C. The data for EDAB show approximately a slope of −1 at low q, which implies $I \sim q^{-1}$ in this region. This scaling relationship is consistent with the presence of cylindrical structures, *i.e.*, WLMs. In comparison, the scattering from PAM is typical of that from flexible polymers in solution; thus, the curves have a different shape at low q. Moreover, the scattering intensity is significantly lower for the PAM compared to the WLMs. This is because the WLMs have a much larger cross-sectional radius (few nm; see below) compared to the atomic radii of the polymer chains.

Regarding the chain dimensions, we expect the EDAB WLMs to be microns in length (as noted in Fig. 5), which is too large to be resolved by SANS. Thus, SANS only allows us to access a

portion of the overall micellar chains. For this reason, we cannot obtain the micellar contour length L by fitting a model to the SANS data. However, we can accurately determine the radius R_{core} of the WLMs in a model-free manner using a cross-sectional Guinier plot,[1,27] *i.e.*, a plot of $qI(q)$ *vs.* q. This plot gives a straight line for WLMs, and from the slope, the radius can be determined. For EDAB WLMs at 25 °C, we calculate a radius R_{core} of 29 Å, which is consistent with previous reports.[4] In principle, it is possible to determine other parameters for the WLMs such as their persistence length l_p by fitting the SANS data to a flexible-cylinder model; however, such modeling did not give us consistent results and the fits are hence not shown.

Regarding the effect of temperature, the SANS spectra for the EDAB WLMs show only a slight decrease in intensity at low q when temperature is increased from 25 to 85 °C. This is suggesting that the micelles are too long even at 85 °C to be resolved by SANS. Note that, although the contour length L of WLMs is expected to decrease exponentially with temperature, EDAB still gives rise to micron-long WLMs at 85 °C (as seen from Fig. 5). In the case of the PAM solution, an increase in temperature from 25 to 85 °C causes a slight increase in low-q scattering intensity and also a change in the shape of the curve. We can fit the PAM data to a model suggested by Hammouda that combines a Lorentzian term with a second term that captures the uptick at very low q. However, the parameters from this model cannot be easily interpreted in terms of structural dimensions like the PAM chains' persistence length l_p; hence the model fits are not shown.

Discussion: EDAB WLMs *vs.* PAM chains

Our studies have revealed many interesting aspects. First, we find that both EDAB WLMs as well as the UHMW chains of the water-soluble PAM are efficient thickeners of water. At 25 °C, the overlap concentration C^* at which the viscosity begins to shoot up is about 0.04 wt% for EDAB and about 0.1 wt% for PAM. Also, the zero-shear viscosity η_0 is comparable for a 1.00 wt% EDAB and a 2.50 wt% PAM solution (both are ~40 000 mPa s, *i.e.*, 40 000 times the viscosity of water, which is ~1 mPa s). These data indicate that EDAB is even more potent as a thickener than the PAM at room temperature. In other words, WLMs of a C_{22}-tailed surfactant are comparable to ultra-long polymers ($M_w > 10^7$) in terms of their rheology-modifying ability. This is a point that has been conceptually stated before, but ours is the first experimental study to validate it. Another point to emphasize is that the thickening of both EDAB and PAM are preserved up to very high temperatures. We focused on the rheology at 85 °C: at this temperature, the 1.00 wt% EDAB solution has a relaxation time τ_R of ~3 s and an η_0 of ~ 6000 mPa s while the 2.50 wt% PAM solution has a τ_R of ~0.3 s and an η_0 of ~10 000 mPa s. That is, both these samples are substantially viscous and viscoelastic even at this elevated temperature. Our study also shows that at 85 °C, EDAB WLMs are viscoelastic and Maxwell fluids while the PAM is viscoelastic, but not a Maxwell fluid.

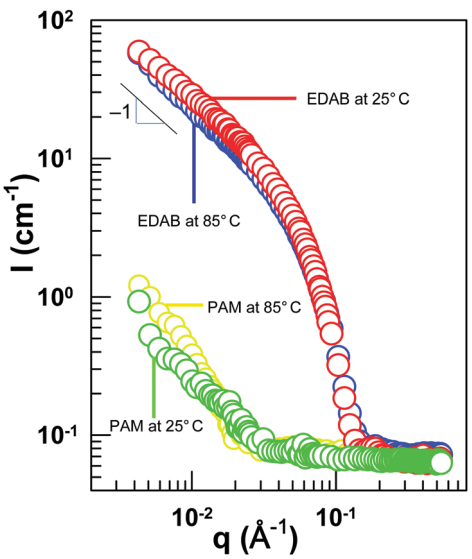

Fig. 6 SANS spectra (intensity I *vs.* wave-vector q) for 2.50 wt% PAM and 1.00 wt% EDAB in D_2O at 25 and 85 °C.

From our studies, we were able to extract some structural and dynamic parameters for EDAB WLMs and PAM chains. Further parameters can be found from the literature or through additional experiments. First, the persistence length l_p of PAM chains has been reported by Starchev *et al.*[28] to be about 0.9 nm. Also, since the length of polymers is invariant with concentration, we can conduct static light scattering on our PAM in very dilute solution. This yields an estimate for the radius of gyration R_g of a single PAM chain (coil) to be 61 nm (Fig. S10, ESI†). Assuming that the PAM chains are random, Gaussian objects, we can apply the following well-known relationship between R_g, l_p and the contour length L:[29]

$$R_g \cong \sqrt{\frac{Ll_p}{3}} \quad (6)$$

Using eqn (6), we estimate the contour length L of our UHMW polymer chains to be 12.4 μm. This is an extremely high value, as expected. Note that the L of EDAB WLMs cannot be measured in a similar manner because L will decrease upon dilution. Nevertheless, given the comparable rheology, we expect the WLMs existing in a 1.00 wt% EDAB sample to also be of similar length (*i.e.*, >10 μm) at 25 °C. This is also consistent with the cryo-TEM image of this sample in Fig. 5A.

Regarding the persistence length l_p of EDAB WLMs, previous estimates of l_p for WLMs in the literature have yielded values from 10 to 50 nm[30–32] (most were based on cationic C_{16}-tailed surfactants). Generally, the l_p of a filament has two contributions: one from the backbone and the other from the charge along the filament. Since the EDAB WLMs are zwitterionic, the contribution from charge should be low. However, l_p also increases with the filament radius (~R_{core}^4) and since EDAB is C_{22}-tailed, this contribution will be higher than for C_{16}-tailed WLMs. Thus, we estimate that l_p must be at least ~20 nm for EDAB WLMs.

Putting these aspects together, a comparison between EDAB WLMs and PAM chains is shown schematically in Fig. 7, along with their dynamic rheology at 85 °C. Both the WLMs and the polymer chains form transient networks at this temperature.

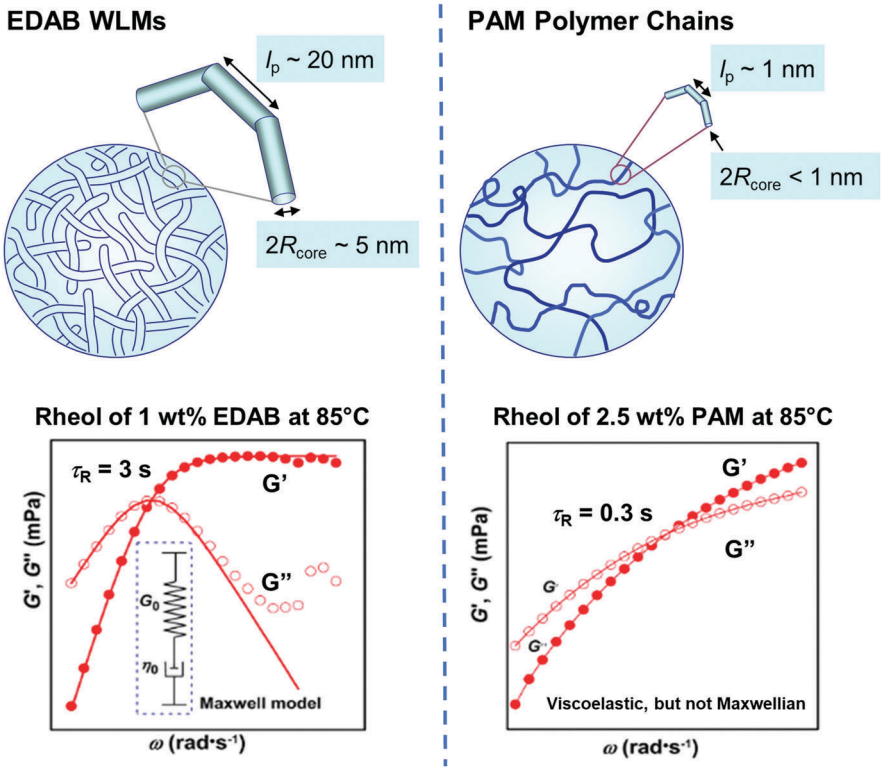

Fig. 7 Comparison of EDAB WLMs and PAM polymer chains. The physical parameters underlying each type of structure are shown in the schematics. The WLMs are thicker than the polymer chains, *i.e.*, their core radii R_{core} are much larger since they are formed by EDAB molecules in a cylindrical arrangement. In turn, the WLM filaments are much stiffer than the polymer chains, *i.e.*, their persistence length l_p is also much larger. Both the WLMs and the PAM chains form transient networks at 85 °C. The rheology of these networks is compared in the plots. The WLMs show the response of a Maxwell fluid, with an overall relaxation time τ_R of 3 s. The PAM solution is a viscoelastic, non-Maxwellian fluid with a relaxation time τ_R of 0.3 s.

As expected, the key differences between the structures are in the cross-sectional radius R_{core} and the persistence length l_p, both of which are significantly larger for the WLMs compared to the PAM chains. The PAM chains are expected to relax from their transient network by reptation alone (this will be true regardless of temperature), and so their observed relaxation time τ_R = 0.3 s is also their reptation time. The WLMs at this temperature show Maxwellian rheology, which implies that they will relax by two modes: reptation, with a timescale τ_{rep} and breaking-recombination with a timescale τ_b.[11] We estimated $\tau_b \sim 0.1$ s and $\tau_{rep} \sim 90$ s; in turn, the observed relaxation time τ_R = 3.0 s is the geometric mean of these two quantities, as per eqn (5). These calculations imply that the WLMs take a much longer time to reptate compared to the ultra-long PAM chains. A possible reason for this discrepancy was suggested recently by Raghavan and Douglas,[33] which is that the entanglements between semiflexible WLMs have a different character compared to those between flexible polymer chains. If this hypothesis is correct, it would also help to explain why the EDAB WLMs show gel-like rheology at low temperatures, unlike the PAM sample.

Conclusions

We have conducted the first direct comparison between WLMs and an UHMW polymer as aqueous rheology modifiers. A long (C_{22}) tailed zwitterionic surfactant EDAB was chosen to form the WLMs while nonionic PAM with a M_w of 1.2×10^7 Da was selected as the polymer. Both types of chains are efficient at thickening saline water at 25 °C. When heated, both the WLM and polymer samples are able to retain significant viscosity at 85 °C. The dynamic rheology of the EDAB WLMs at 85 °C follows the Maxwell model, indicating that the sample is a viscoelastic fluid with a single relaxation time. The PAM sample at 85 °C is also viscoelastic, but it exhibits a spectrum of relaxation times. Both the WLMs and the polymer chains show an exponential reduction in their zero-shear viscosity (Arrhenius behavior) at moderate to high temperatures. The slope of the Arrhenius plot (corresponding to the flow activation energy) is much higher for the WLMs, indicating that they are more sensitive to temperature. Microstructural characterization of the above samples by cryo-TEM and SANS confirm the larger radius R_{core} and the longer persistence length l_p of WLMs compared to the polymer chains. In short, WLMs are thicker and stiffer than polymers.

Conflicts of interest

There are no conflicts to declare.

Acknowledgements

This work was supported by the opening fund from the State Key Laboratory of Polymer Materials Engineering (sklpme2014-2-06),

and the Natural Science Foundation of China (No. 21773161 and 21173207). We acknowledge NIST NCNR for facilitating the SANS experiments performed as part of this work.

References

1 C. A. Dreiss, *Soft Matter*, 2007, **3**, 956–970.
2 Z. Chu, C. A. Dreiss and Y. Feng, *Chem. Soc. Rev.*, 2013, **42**, 7174–7203.
3 J. Yang, *Curr. Opin. Colloid Interface Sci.*, 2002, **7**, 276–281.
4 R. Kumar, G. C. Kalur, L. Ziserman, D. Danino and S. R. Raghavan, *Langmuir*, 2007, **23**, 12849–12856.
5 S. R. Raghavan and E. W. Kaler, *Langmuir*, 2001, **17**, 300–306.
6 Z. Chu, Y. Feng, X. Su and Y. Han, *Langmuir*, 2010, **26**, 7783–7791.
7 Y. Han, Y. Feng, H. Sun, Z. Li, Y. Han and H. Wang, *J. Phys. Chem. B*, 2011, **115**, 6893–6902.
8 M. E. Cates, *J. Phys.*, 1988, **49**, 1593–1600.
9 V. Schmitt, F. Lequeux, A. Pousse and D. Roux, *Langmuir*, 1994, **10**, 955–961.
10 P. G. de Gennes, *J. Chem. Phys.*, 1971, **55**, 572–579.
11 M. E. Cates, *Macromolecules*, 1987, **20**, 2289–2296.
12 R. G. Larson, *The Structure and Rheology of Complex Fluids*, Oxford University Press, New York, 1998.
13 W. W. Graessley, *Polymeric Liquids & Networks: Dynamics and Rheology*, Taylor & Francis, New York, 2008.
14 F. Kern, R. Zana and S. J. Candau, *Langmuir*, 1991, **7**, 1344–1351.
15 L. Ziserman, L. Abezgauz, O. Ramon, S. R. Raghavan and D. Danino, *Langmuir*, 2009, **25**, 10483–10489.
16 L. J. Magid, *J. Phys. Chem. B*, 1998, **102**, 4064–4074.
17 S. J. Candau, E. Hirsch and R. Zana, *J. Colloid Interface Sci.*, 1985, **105**, 521–528.
18 W.-M. Kulicke, R. Kniewske and J. Klein, *Prog. Polym. Sci.*, 1982, **8**, 373–468.
19 D. Feng, Y. Zhang, Q. Chen, J. Wang, B. Li and Y. Feng, *J. Surfactants Deterg.*, 2012, **15**, 657–661.
20 X. Li, Z. Xu, H. Yin, Y. Feng and H. Quan, *Energy Fuels*, 2017, **31**, 2479–2487.
21 T. G. Mezger, *The Rheological Handbook: For Users of Rotational and Oscillatory Rheometers*, 2nd revised edn, 2006, ch. 8, p. 169.
22 Y. Hu, S. Q. Wang and A. M. Jamieson, *Macromolecules*, 1995, **28**, 1847–1853.
23 R. H. Colby, *Rheol. Acta*, 2010, **49**, 425–442.
24 M. E. Cates and S. J. Candau, *J. Phys.: Condens. Matter*, 1990, **2**, 6869.
25 R. Granek and M. E. Cates, *J. Chem. Phys.*, 1992, **96**, 4758–4767.
26 Y. Talmon, in *Giant Micelles: Properties and Applications*, ed. R. Zana and E. W. Kaler, 2007, ch. 5, pp. 163–178.
27 J. S. Pedersen, L. Cannavacciuolo and P. Schurtenberger, in *Giant Micelles: Properties and Applications*, ed. R. Zana and E. W. Kaler, 2007, ch. 6, pp. 179–223.
28 K. Starchev, J. Sturm and G. Weill, *Macromolecules*, 1999, **32**, 348–352.
29 H. Yamakawa, in *Modern Theory of Polymer Solutions*, ed. H. Yamakawa, 1971, ch. 2, pp. 5–52.
30 W.-R. Chen, P. D. Butler and L. J. Magid, *Langmuir*, 2006, **22**, 6539–6548.
31 L. Arleth, M. Bergström and J. S. Pedersen, *Langmuir*, 2002, **18**, 5343–5353.
32 M. Bergström and J. S. Pedersen, *Langmuir*, 1999, **15**, 2250–2253.
33 S. R. Raghavan and J. F. Douglas, *Soft Matter*, 2012, **8**, 8539–8546.

Electronic Supplementary Information for

Wormlike Micelles versus Water-Soluble Polymers as Rheology-Modifiers: Similarities and Differences

Ji Wang,[a,c] Yujun Feng,*[,a,b] Niti R. Agrawal,[d] Srinivasa R. Raghavan[d]

[a] Chengdu Institute of Organic Chemistry, Chinese Academy of Sciences, Chengdu 610041, People's Republic of China.

[b] Polymer Research Institute, State Key Laboratory of Polymer Materials Engineering, Sichuan University, Chengdu 610065, People's Republic of China.

[c] University of the Chinese Academy of Sciences, Beijing 100049, People's Republic of China.

[d] Department of Chemical & Biomolecular Engineering, University of Maryland, College Park, Maryland, 20742-2111, USA

Corresponding authors: e-mail: yjfeng@scu.edu.cn.

Preparation of poly-(2-(dimethyl(3-(acrylamido)propyl ammonium acetate)

Synthesis of Monomer

Following the pathway listed in Scheme S1, the typical experimental procedure for the synthesis is as follows: In a 0.25 L flask equipped with a stirrer, a cooler, and a thermometer, 0.05 mol (8.34 g) *N,N*-dimethylaminopropyl acrylamide and dried acetonitrile were charged under a N_2 atmosphere and the contents were stirred at 55 ºC. Subsequently, 0.08 mol (9.30 g) sodium chloroacetate was added. Following the addition, the mixture was stirred and allowed to stand at the same temperature for 24 h. The solvent was accumulated by filtration, washed with dry ether for several times, and dried under reduced pressure to obtain *N, N*-dimethy ((acrylamido)propyl) ammonium acetate (DMAPAAC). Yield: 9.15 g, 80%.

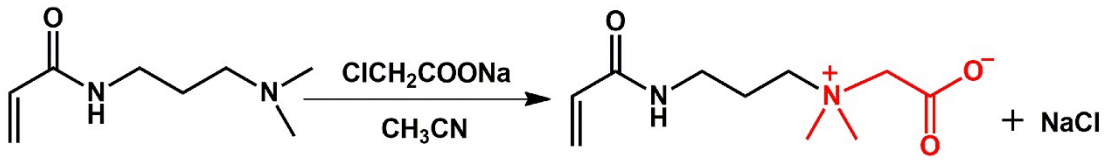

DMAPMA DMAPAAC

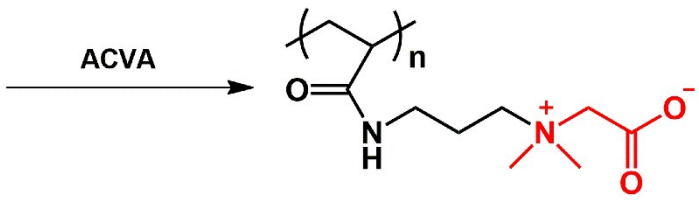

PDAPAA

Scheme S1. The protocol for the synthesis of poly-(2-(dimethyl(3-(acrylamido)propyl ammonium acetate).

Polymerization of Monomer

0.02 mol (4.28 g) The monomer (DMAPAAC) and 0.2 mol % (0.01 g) of 4,4'-azobis(4-cyanovaleric acid) (ACVA) were introduced into a 100 mL ampule. To this, 50 mL of distilled water was added to make a 0.4 M aqueous solution. The ampule contents were then flushed with argon, sealed in vacuum, and then placed in a temperature bath for 24 h. Next, the polymer solutions were precipitated with acetone, lyophilized for 24 h. A dried, brittle, and white solid polymer was subsequently obtained. The structure of the poly-(2-(dimethyl(3-(acrylamido)propyl ammonium acetate) (PDAPAA) was confirmed by ^{1}H NMR spectroscopy (Figure S1), and its molecular weight was determined by gel permeation chromatography (Figure S2).

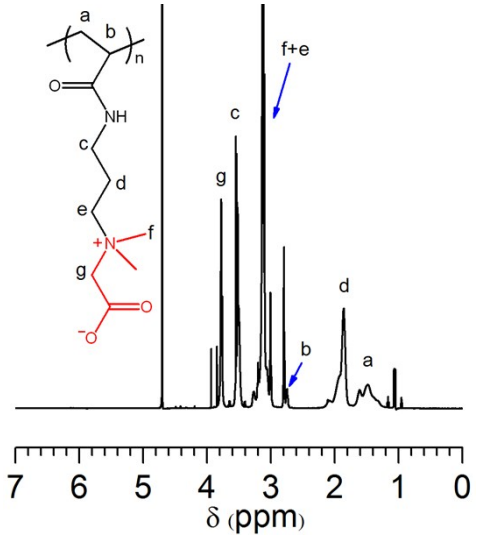

Figure S1. ^{1}H NMR spectrum of poly-(2-(dimethyl(3-(acrylamido)propyl ammonium acetate) in D_2O.

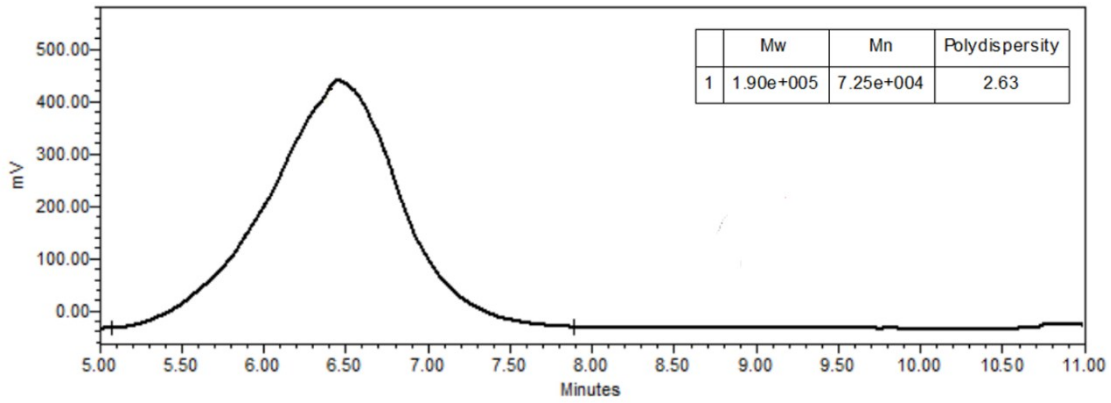

Figure S2. GPC trace of poly-(2-(dimethyl(3-(acrylamido)propyl ammonium acetate).

Characterization of EDAB

The structure and purity of EDAB was confirmed by ^{1}H NMR spectroscopy (Figure S3) and high performance liquid chromatography (HPLC) (Figure S4), respectively.

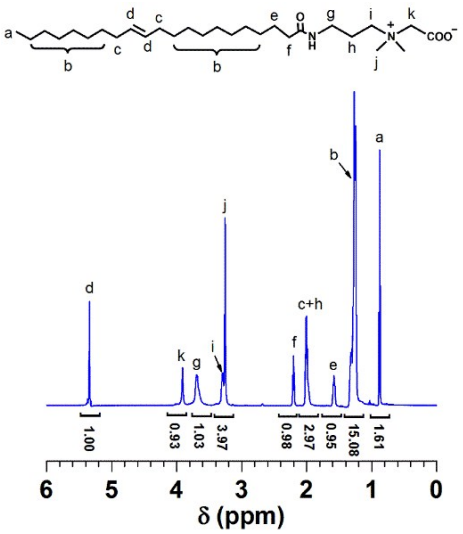

Figure S3. ^{1}H NMR spectrum of erucyl dimethyl amidopropyl betaine (EDAB) in CD_3Cl.

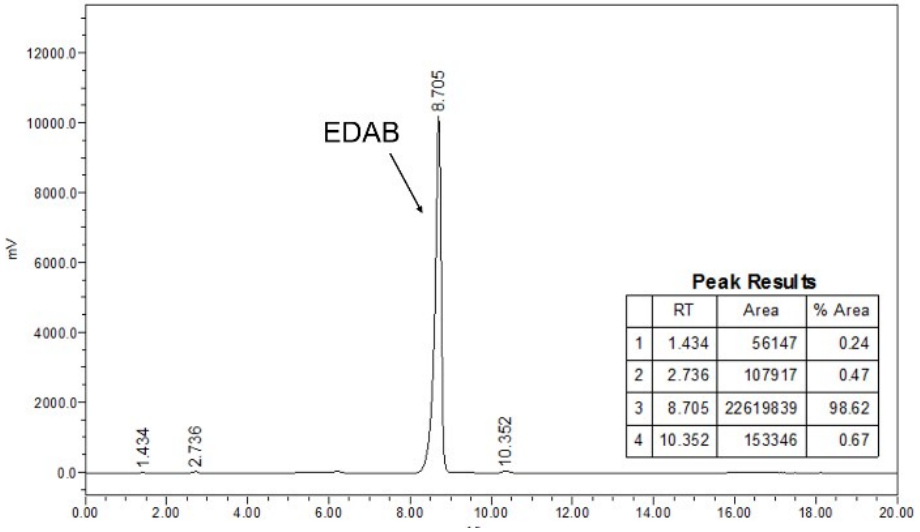

Figure S4. HPLC result of erucyl dimethyl amidopropyl betaine (EDAB).

Determination of chloride ion content in EDAB with ion chromatography

The chloride ion content in EDAB powder was determined by ion chromatography. EDAB solution (0.5 mg·mL^{-1}) was prepared by dissolving surfactant powders in deionized water, followed by gentle agitation while mildly heating. When completely solubilized at high temperatures, the solution was cooled, and then left to stand overnight to measurements.

Ion chromatography (IC) was performed using Dionex Ion Analyzer (Dionex, Sunnyvale, CA, USA) equipped with a GP40 gradient pump, an ED40 electrochemical detector, and an AS40 autosampler. One Dionex, 4 × 210 mm anion-exchange columns was tested: Ion-Pac AS14. 2 mM phthalic acid/10% acetone (pH 5.0) was used as the mobile phase. Flow rate was varied from 1.0 mL/min to 1.2 mL/min. The detector stabilizer temperature was set at 30 °C with temperature compensation of 1.7%/°C. Anion suppressor current was set to 300 mA. The injection volume was 20 μL. A series of standard solutions with increasing values of Cl^- were used for the calibration graph for Cl^- determination. The plot of the peak area versus the chloride concentration was found to be linear up to 100 mg/L of NaCl, with the following linear

regression equation:

$$y = 0.059 + 0.727x \qquad (r^2 = 0.9999)$$

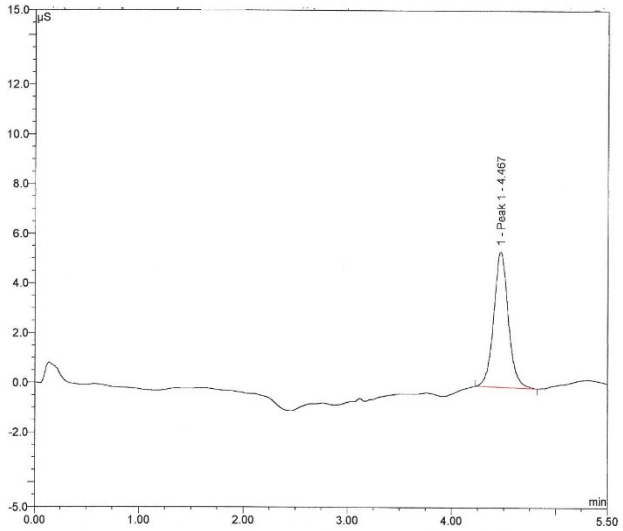

Figure S5. Ion chromatographic result of standard solution of Cl^-.

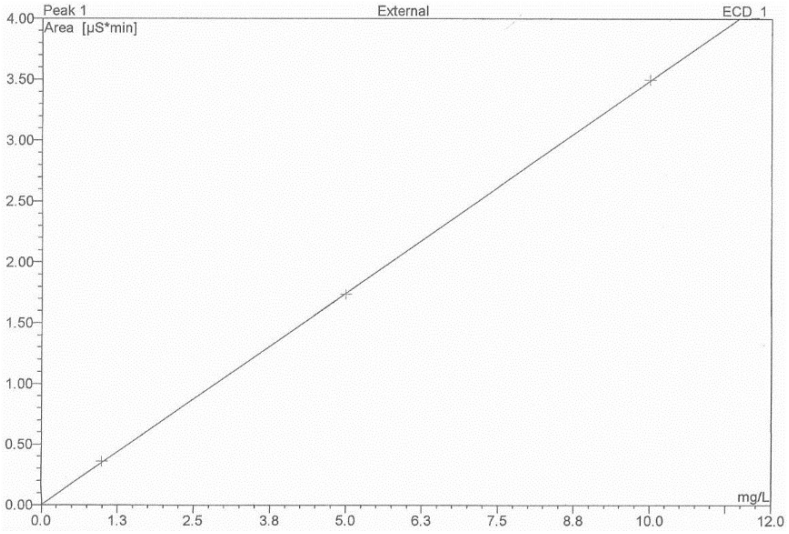

Figure S6. Calibration curves of Cl^- obtained by IC.

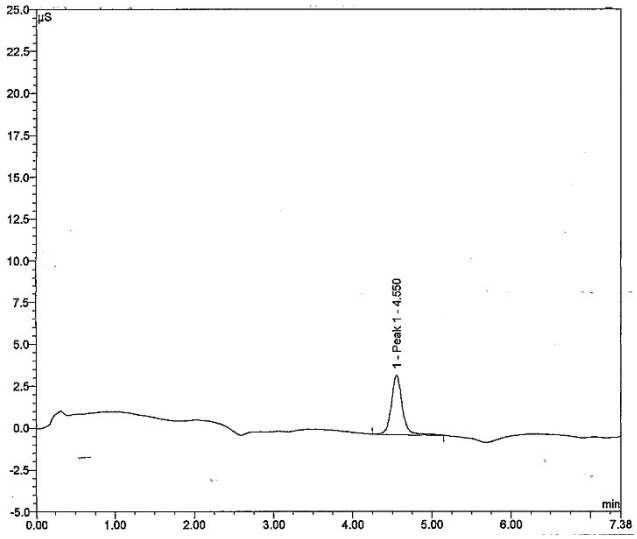

Figure S7. IC result of erucyl dimethyl amidopropyl betaine (EDAB).

Additional Rheological results

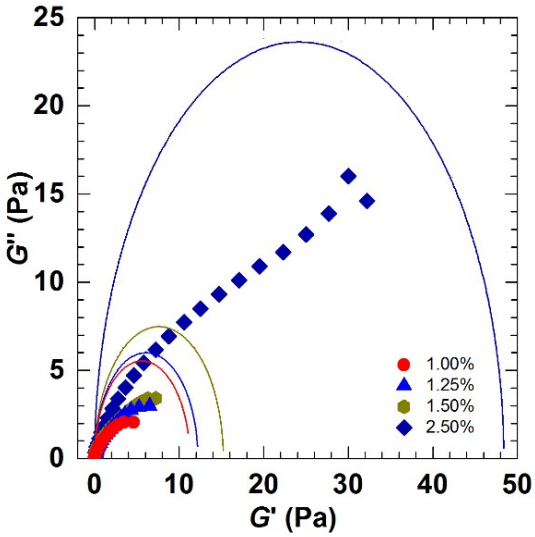

Figure S8. Experimental Cole-Cole plots for PAM saline aqueous solution at different concentrations. The solid line represents the osculating semicircle at the origin.

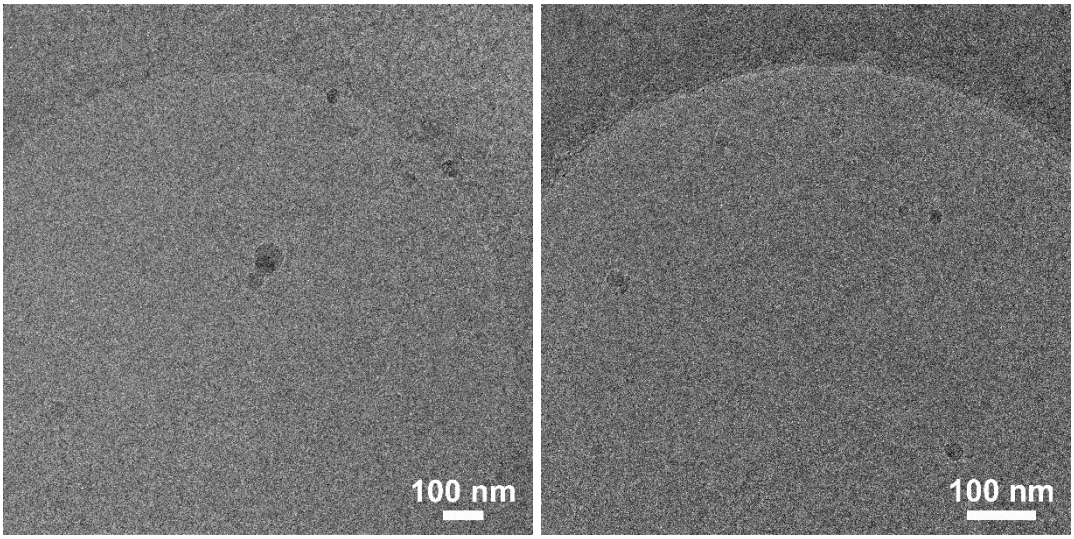

Figure S9. Cryo-TEM micrographs of 2.50 wt % PAM saline aqueous solution at 25 ºC (A) and 85 ºC (B).

Static light scattering

The radius of gyration (R_g) of samples were measured in 0.5 M NaCl by static light scattering with a Brookhaven Instrument equipped with BI-200SM goniometer and a BI-TurboCorr digital correlation. A solid-state laser polarized at the vertical direction (532 nm, 100 mW) was used as light source. The light scatting measurements were carried out at 25 ºC. Toluene was used as a reference standard. The scattering angle θ was varied from 30 to 150°. The experiments were carried in a dilute polymer concentration where intermolecular associations can be neglected. Solvents were filtered through Durapore (Millipore) 0.20 μm membrane, polymer solutions were filtered through Durapore 0.45 μm membrane. The refractive index increment was measured at the same wavelength on a brice-Phoenix differential refractometer.

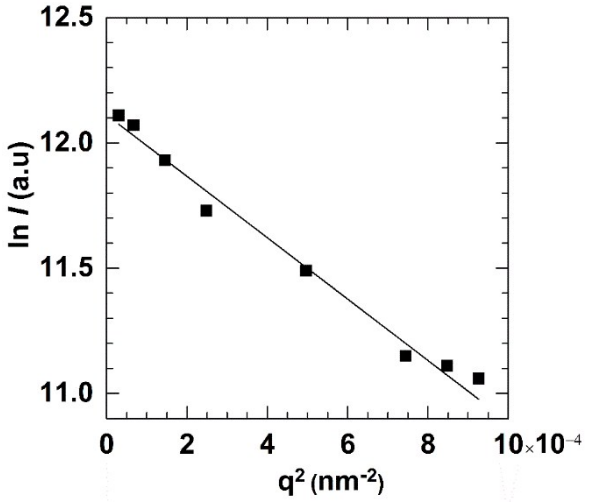

Figure S10. Guinier plot of PAM in 0.5 M NaCl at 25 °C. R_g of a single PAM chain is about 61 nm.